



# An Analytical Substructure Method for the Analysis of Vibration Characteristics on Conical-Cylindrical-Spherical Combined Shells in Vacuum

Meixia CHEN<sup>1</sup>; Kun XIE<sup>2</sup>; Jianhui WEI<sup>3</sup>; Naiqi DENG<sup>4</sup>

<sup>1,2,3,4</sup> Huazhong University of Science and Technology, China

<sup>1</sup> The University of Western Australia, Australia

## ABSTRACT

In this paper a new semi-analytic numerical method *i.e.* Analytical Substructure Method (ASM) is established to study the vibration characteristics of conical-cylindrical-spherical combined shell with arbitrary boundary conditions in vacuum. First, according to the structure types, the whole structure is divided into substructures: conical shell, annular circular plates, bulkheads, cylindrical shells, open spherical shell. Second, by using power series method, annular circular plate theory, and wave propagation method and by introducing auxiliary functions, the dynamic equations of the substructures are formed respectively. Then using the boundary conditions and the displacement and force continuity conditions between the substructures, the dynamic equation of the whole structure is established. Finally, the vibration characteristics of the structure are obtained. By comparison with computational results obtained from a finite element method, the accuracy and the efficiency of ASM are verified. Three common boundary conditions of the structure are discussed in numerical analysis. The paper demonstrates that ASM is applicable for complex structures with all tested boundary conditions, providing a new approach and idea to study the vibration characteristics of complex combined shells.

Keywords: Analytical Substructure Method, Conical-cylindrical-spherical combined shell, Vibration characteristics, Arbitrary boundary conditions

I-INCE Classification of Subjects Number(s): 54.3, 75.9, 42

## 1. INTRODUCTION

Conical-cylindrical-spherical(C-C-S) combined shell is the simplified model of underwater vessel. The prediction of vibration characteristics of underwater vessel is regarded as the theoretical foundation and important criterion for quantitative acoustic design and noise control. In order to overcome the structural boundary errors which would be brought by single segment models, The C-C-S combined shell model should be built and solved uniformly. At present the prediction methods for vibration characteristics of underwater vessel are analytical method (displacement method, energy method and wave propagation method), numerical simulation (finite element method (FEM) / boundary element method (BEM)) and model testing. Compared with the numerical method and testing method, analytical method which is fast in solving speed, less cost, easy to reveal the mechanism and suitable for multi-scheme calculation and optimization, is mostly attractive.

Due to the structure complexity of combined shell, using completely analytical method to study would be very difficult. Therefore the main theoretical method on C-C-S combined shell is a semi-analytical and semi-numerical method at present. In 2008, the active control on radiated sound pressure of C-C-S combined shell in low frequencies was researched by Pan et. al. (1), who simulated propeller excitation by exerting an axial exciting force on the end of the conical shell. The axisymmetric vibration of  $n = 0$  was considered, but the bending vibration of  $n > 0$  was not considered.

---

<sup>1</sup> chenmx26@hust.edu.cn

<sup>2</sup> xiekun79@163.com

<sup>3</sup> wjhust@hust.edu.cn

<sup>4</sup> dengnq@hust.edu.cn

In 2009, Caresta and Kessissoglou (2) studied vibro-acoustic characteristics of multi-segmental cylindrical shell by axial excitation in low frequencies. In their work, the stiffeners were used by orthotropic method that the weight of stiffeners were even distributed in the shell surface, the stiffness of stiffeners was acted as orthotropic stiffness of the shell. The orthotropic method of stiffeners is suitable for conditions with the equal spacing, small size, and dense stiffeners. In 2010, the vibration characteristics of conical-cylindrical combined shell were reported by Caresta and Kessissoglou (3). The cylindrical shell and conical shell respectively used wave method and the power series method. Then based on the continuity conditions of the conical-cylindrical junction, the coupled vibration equation of the combined shell was established. The stiffeners were still used by orthotropic method. In 2012, Qu et. al. (4) investigated the vibration characteristics of conical-cylindrical combined shell with different boundary conditions by energy method and improved difference method. Due to the coupling of structures, the whole energy equation needs solve uniformly. The calculated speed increased rapidly with the complexity of the structure. In addition, the mechanism analysis was not easy to conduct by difference method.

On the basis of the above literatures, and in order to solve the problems existing in the previous researches, using the conception of substructure division in FEM and the thought of “the structure displacement function needs satisfy its dynamic equation” in traditional analytical method for references, a new semi-analytical and semi-numerical method named Analytical Substructure Method (ASM) is formed in this paper. The principle of ASM is to divide the C-C-S combined shell into different substructures according to the type of structures (beams, plates, shells, etc.). Each substructure displacement function needs to satisfy the corresponding dynamic equation. Boundary conditions and continuity conditions between substructures are used to form the final dynamic stiffness matrix to calculate the vibration responses of the whole structure. ASM is suitable for the condition of structural parameters varying along the length direction. This method has the advantages of division flexibility exists in FEM, solution rapidity and easy to reveal the mechanism exist in analytic method. The stiffeners act as discrete components processing (5) in the paper, and would be more correct than as orthotropic processing in previous studies. Furthermore, the method can deal with axisymmetric vibration, as well as non-axisymmetric bending vibration. Thus, ASM is a very effective method for solving the vibration characteristics of C-C-S combined shell. In the numerical analysis of the paper, by comparison with computational results obtained from FEM, the correctness and the affectivity of ASM are verified. Then the influences of three boundary conditions of combined shell are discussed in the end.

## 2. BASIC CONCEPT AND PROCEDURE OF ASM

In this paper, ASM is developed to analyze vibration characteristics of ring stiffened C-C-S combined shell for arbitrary boundary conditions shown in Figure 1. Firstly, the C-C-S combined shell is divided into different substructures: conical shell, ordinary ribs, large frame rib, bulkheads, cylindrical shells, open spherical shell. The cylindrical shell and the conical shell, the motions of which are described by the equations of Donnell-Mushtari theory, are divided into substructures according to the positions of discontinuities. Ordinary ribs, large frame rib and bulkheads are divided into separate substructures, the motions of which are described by the equations of circular plates. For open spherical shell, the five equations of motions describing the spherical shell are simplified to three uncoupling equations by introducing auxiliary functions. The dynamic field variables in the substructures of cylindrical shells are expanded by wave functions given in references (5, 6, 7) and those in substructures of ordinary ribs, large frame rib and bulkheads are expanded by wave functions given in references (8). The displacements in substructures of the conical shell are expanded in the form of power series given in references (3, 9, 10, 11). The displacements in substructures of spherical shell can be presented in the form of combinations of Bessel Functions by solving three uncoupling equations in reference (12). Then equilibrium and compatibility conditions between different substructures are established. Combined with boundary conditions of the C-C-S combined shell, the final matrix can be formed to solve the vibration displacements.

### 2.1 Substructure Division of C-C-S Combined Shell

Substructure divisions of C-C-S combined shell are shown in Figure 2. According to the structure types and the position of excitation force, the whole structure is divided into different substructures: conical shell, ordinary ribs, large frame rib, bulkheads, cylindrical shells, open spherical shell. In Figure 1, five bulkheads divide the whole structure into six sections: one conical shell section, four

cylindrical shell sections, and one spherical shell section. Thus there are 17 ordinary ribs in conical shell section, 75 ordinary ribs, 5 bulkheads, one large frame rib in four cylindrical shell sections, and none ribs in open spherical shell. As the excitation force is located just on a certain ordinary rib position, no additional substructure need to add in the total substructures. The numbers of substructures are shown in Table.1. The total number of stiffener substructures is  $N_r = N_{r1} + N_{r2} + N_{r3} + N_{r4} = 98$ , and the total number of shell substructures is  $N_s = N_{s1} + N_{s2} + N_{s3} = 99$ . The relationship between the number of stiffener substructures and the number of shell substructures are as follows:  $N_s = N_r + 1$ .

Table 1 – The numbers of substructures in C-C-S combined shell

Description of section	Description of substructures	Number of substructures
One conical shell section	ordinary ribs	$N_{r1} = 17$
	<b>conical shells</b>	<b><math>N_{s1} = 18</math></b>
Four cylindrical shell sections	ordinary ribs	$N_{r2} = 75$
	large frame rib	$N_{r3} = 1$
	bulkheads	$N_{r4} = 5$
	<b>cylindrical shell</b>	<b><math>N_{s2} = 80</math></b>
One spherical shell section	<b>open spherical shell</b>	<b><math>N_{s3} = 1</math></b>
<b>Total number of Shell substructures</b>		<b><math>N_s = N_{s1} + N_{s2} + N_{s3} = 99</math></b>

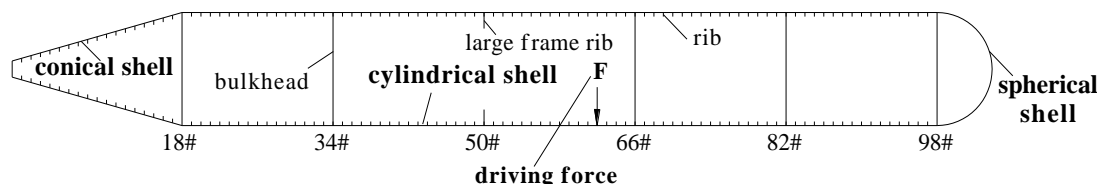
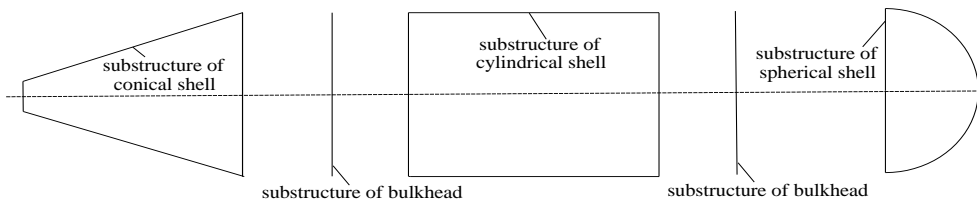
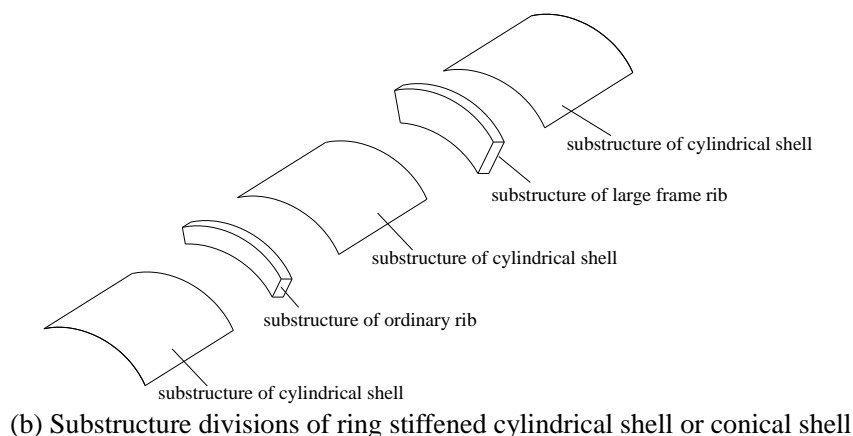


Figure 1 – Sketch of conical-cylindrical-spherical combined shell



(a) Sections of C-C-S combined shell



(b) Substructure divisions of ring stiffened cylindrical shell or conical shell

Figure 2 – Substructure divisions of C-C-S combined shell

## 2.2 Equations of Substructures

### 2.2.1 Equations of Cylinder Shell

In this work, Donnell-Mushtari equations are used to describe the motions of cylindrical shell as follows (5):

$$\begin{aligned}
\frac{\partial^2 u}{\partial x^2} + \frac{1-\nu}{2} \frac{\partial^2 u}{\partial \phi^2} + \frac{1+\nu}{2} \frac{\partial^2 v}{\partial x \partial \phi} + \nu \frac{\partial w}{\partial x} - \frac{\rho a^2 (1-\nu^2)}{E} \frac{\partial^2 u}{\partial t^2} &= 0 \\
\frac{1+\nu}{2} \frac{\partial^2 u}{\partial x \partial \phi} + \frac{\partial^2 v}{\partial \phi^2} + \frac{1-\nu}{2} \frac{\partial^2 v}{\partial x^2} + \frac{\partial w}{\partial \phi} - \frac{\rho a^2 (1-\nu^2)}{E} \frac{\partial^2 v}{\partial t^2} &= 0 \\
\nu \frac{\partial u}{\partial x} + \frac{\partial v}{\partial \phi} + w + k \left( \frac{\partial^4 w}{\partial x^4} + 2 \frac{\partial^4 w}{\partial x^2 \partial \phi^2} + \frac{\partial^4 w}{\partial \phi^4} \right) + \frac{\rho a^2 (1-\nu^2)}{E} \frac{\partial^2 w}{\partial t^2} &= 0
\end{aligned} \tag{1}$$

The radius of the cylindrical shell is designated by  $a$ , and the thickness by  $h$ ,  $k=h^2/12a^2$ ,  $u$ ,  $v$ , and  $w$  are respectively the axial, circumferential and normal displacements. The axial and circumferential coordinates are  $x, \phi$ , and  $x = \bar{x}/a$  is the non-dimensional axial coordinates. The mass density of the cylindrical shells is designated by  $\rho$ , Young's modulus by  $E$  and Poisson ratio by  $\nu$ .

The displacements and the internal forces of the cylindrical shells are expanded as the superposition of eight wave functions and eight undetermined coefficients. The detailed solving process can be found in references (5, 6, 7). The displacements and forces continuity conditions which are used to form the final matrix to calculate the frequency responses of the structure are given in section 2.3.

### 2.2.2 Equations of Ordinary Rib, Large Frame Rib and Bulkhead

The ordinary rib, large frame rib and bulkhead are treated as separate substructures. Their governing equations are the same, all described by the equations of circular plates whose bending and in-plane motions are described in Eq. (2). Annular circular plate with inner radius  $a_1$  and outer radius  $a$  (also the radius of the cylindrical shell) is used to establish the mathematical model of ordinary ribs and large frame rib.  $w_p$ ,  $u_p$  and  $v_p$  are the axial displacement, radial displacement and circumferential displacement of the plate respectively. Circular plate with radius  $a$  is used to establish the mathematical model of bulkheads. The difference between the annular circular plates and the circular plates is that there are no free edges at the inner radius of circular plates.

$$\begin{cases}
\frac{\partial}{\partial r} \left( \frac{\partial u_p}{\partial r} + \frac{u_p}{r} + \frac{1}{r} \frac{\partial v_p}{\partial \theta} \right) - \frac{1-\nu_p}{2r} \frac{\partial}{\partial \theta} \left( \frac{\partial v_p}{\partial r} + \frac{v_p}{r} - \frac{1}{r} \frac{\partial u_p}{\partial \theta} \right) = \frac{\rho_p (1-\nu_p^2)}{E_p} \frac{\partial^2 u_p}{\partial t^2} \\
\frac{1}{r} \frac{\partial}{\partial \theta} \left( \frac{\partial u_p}{\partial r} + \frac{u_p}{r} + \frac{1}{r} \frac{\partial v_p}{\partial \theta} \right) + \frac{1-\nu_p}{2} \frac{\partial}{\partial r} \left( \frac{\partial v_p}{\partial r} + \frac{v_p}{r} - \frac{1}{r} \frac{\partial u_p}{\partial \theta} \right) = \frac{\rho_p (1-\nu_p^2)}{E_p} \frac{\partial^2 v_p}{\partial t^2} \\
\frac{\partial^4 w}{\partial r^4} + 2 \frac{\partial^4 w}{\partial r^2 \partial \theta^2} + \frac{\partial^4 w}{\partial \theta^4} - \frac{\rho_p \omega^2 h_p}{D_p} w_p = 0
\end{cases} \tag{2}$$

where  $D_p = E_p h_p^3 / 12(1-\nu_p^2)$  is the flexural rigidity.  $h_p$  is the plate thickness.  $E_p$ ,  $\rho_p$  and  $\nu_p$  are respectively the Young's modulus, density and Poisson's ratio.

The displacements and the internal forces of the ordinary ribs, large frame rib and bulkheads are expanded as the superposition of the combination of Bessel Functions. The detailed solving process can be found in reference (8). Combined with the displacements and forces continuity conditions of stiffeners (the ordinary ribs, large frame rib or bulkheads) and the shells (cylindrical shells or conical shells) as shown in section 2.3, the final stiffness matrix can be formed.

### 2.2.3 Equations of Conical Shell

The motions of conical shells are described by Donnell-Mushtari equations (10):

$$L_{11}u_c + L_{12}v_c + L_{13}w_c - \frac{1}{c_{cL}^2} \frac{\partial^2 u_c}{\partial t^2} = 0 \quad L_{21}u_c + L_{22}v_c + L_{23}w_c - \frac{1}{c_{cL}^2} \frac{\partial^2 v_c}{\partial t^2} = 0 \quad L_{31}u_c + L_{32}v_c + L_{33}w_c - \frac{1}{c_{cL}^2} \frac{\partial^2 w_c}{\partial t^2} = 0 \tag{3}$$

where  $u_c$ ,  $v_c$  and  $w_c$  are the displacements of conical generatrix direction, circumferential direction and normal direction respectively.  $c_{cL} = [E_c / \rho_c (1-\nu_c^2)]^{1/2}$  is the longitudinal wave velocity of the conical shell.  $L_{ij}$  is the differential operator which is expressed in reference (10).  $E_c$ ,  $\rho_c$  and  $\nu_c$  are respectively the Young's modulus, density and Poisson's ratio of the conical shell.

The displacements of the conical shells are expanded in the form of power series. The detailed solving process can be found in references (3, 9, 10, 11). Combined with the boundary conditions and the displacements and forces continuity conditions of the conical shells as shown in section 2.3, the final matrix can be built.

## 2.2.4 Equations of Spherical Shell

Based on Flügge theory, the five equations describing the spherical shell are simplified to three uncoupling equations by introducing auxiliary functions (12):

$$\begin{aligned}\nabla^2 \psi &= \frac{2}{1-\nu_{sp}} \frac{\lambda_{sp} k_1}{\omega^2} \frac{\partial^2 \psi}{\partial t^2} - \frac{2(1+\nu_{sp})}{E_{sp} h_{sp}} \frac{1}{r_{sp}} S_{,r} \\ k_\delta \nabla^2 \Lambda &= \frac{2}{1-\nu_{sp}} \left[ \frac{\lambda_{sp}}{\omega^2} k_r k_\delta \frac{\partial^2 \Lambda}{\partial t^2} + \frac{6(1-\nu_{sp})}{h_{sp}^2} \Lambda \right] \\ \nabla^6 w_{s,p} + r \nabla^4 w_{s,p} + r^2 \nabla^2 w_{s,p} + r^3 w_{s,p} &= \end{aligned} \quad (4)$$

where  $h_{sp}$  and  $R_{sp}$  are the thickness and radius of the spherical shell.  $r_{sp}$  and  $w_{sp}$  are the radial coordinate and displacement of spherical shell respectively.  $E_{sp}$ ,  $\rho_{sp}$  and  $\nu_{sp}$  are respectively the Young's modulus, density and Poisson's ratio of spherical shell.  $\omega$  is excitation angular frequency.  $\psi$ ,  $\Lambda$  are the introduced auxiliary functions.  $r_1$ ,  $r_2$ ,  $r_3$  and  $T$  are the coefficients that can be seen in reference (12).  $\lambda_{sp}/\omega^2 = \rho_{sp}(1-\nu_{sp}^2)/E_{sp}$ ,  $k_\delta = 6/5$  is average shear coefficient,  $k_l = 1 + h_{sp}^2/(12 R_{sp}^2)$ ,  $k_r = 1 + 3h_{sp}^2/(20 R_{sp}^2)$ ,  $S_{,r} = \partial S/\partial r$ ,  $S = P - F$ , and  $P$ ,  $F$  are the longitudinal and latitudinal loads respectively.

The solutions to the three uncoupling equations can be presented in the form of combinations of Bessel Functions. The detailed solving process can be found in reference (12). The variables of the Bessel Functions can be obtained by solving the three characteristic equations corresponding to the three uncoupling equations. Then combined with the boundary conditions and continuity conditions as shown in section 2.3 the final matrix equation can be obtained.

## 2.3 Boundary Conditions and Continuity Conditions

### 2.3.1 Boundary Conditions

#### 2.3.1.1 The End of Conical Shell

As shown in Figure 3, the conical shells with arbitrary boundary conditions have four displacement constraints and four force or moment constraints, i.e.,

$$u_c = 0, v_c = 0, w_c = 0, \theta_c = 0 \quad \text{and} \quad V_{x,c} = 0, M_{x,c} = 0, N_{x\theta,c} = 0, N_{x,c} = 0 \quad (5)$$

where  $\theta_c$  designates the twisting angle and  $M_{x,c}$ ,  $V_{x,c}$ ,  $T_{x,c}$ ,  $N_{x,c}$  denotes bending moment, transverse shear, tangential shear and axial force per unit length of the conical shell. The displacements and forces' detailed expressions can be found in reference (10). Combination of these eight boundary conditions can present arbitrary boundary conditions. For example:

$$\text{For clamped boundary conditions,} \quad u_c = v_c = w_c = \theta_c = 0 \quad (6)$$

$$\text{For shear diaphragm boundary conditions,} \quad v_c = w_c = V_{x,c} = M_{x,c} = 0 \quad (7)$$

$$\text{For free boundary conditions,} \quad V_{x,c} = M_{x,c} = N_{x\theta,c} = N_{x,c} = 0 \quad (8)$$

#### 2.3.1.2 The End of Spherical Shell

As shown in Figure 3, for the open end of the spherical shell, there are only five unknown displacement function coefficients. At its open end there are five displacement boundary conditions and five force boundary conditions as follows:

$$u_{r_{\phi sp}} = u_{\theta_{\phi sp}} = w_{\phi sp} = \beta_{\theta_{\phi sp}} = \beta_{r_{\phi sp}} = 0 \quad \text{and} \quad N_{r_{\phi sp}} = N_{r_{\phi sp} \theta_{\phi sp}} = M_{r_{\phi sp}} = M_{r_{\phi sp} \theta_{\phi sp}} = Q_{r_{\phi sp}} = 0. \quad (9)$$

Parameters in Eq. (9) are displacements and internal forces of spherical shell shown in Figure 3. The displacements and forces' detailed expressions can be found in reference (12). Combination of these boundary conditions can express arbitrary boundary conditions. For example:

$$\text{For clamped boundary conditions,} \quad u_{r_{\phi sp}} = u_{\theta_{\phi sp}} = w_{\phi sp} = \beta_{r_{\phi sp}} = 0$$

$$\text{For shear diaphragm boundary conditions,} \quad u_{\theta_{\phi sp}} = w_{\phi sp} = M_{r_{\phi sp}} = Q_{r_{\phi sp}} = 0$$

$$\text{For free boundary conditions,} \quad N_{r_{\phi sp}} = N_{r_{\phi sp} \theta_{\phi sp}} = M_{r_{\phi sp}} = Q_{r_{\phi sp}} = 0$$

### 2.3.2 Continuity Conditions

As shown in Figure 3, continuity conditions of C-C-S combined shell should be unified to the cylindrical coordinates to describe.

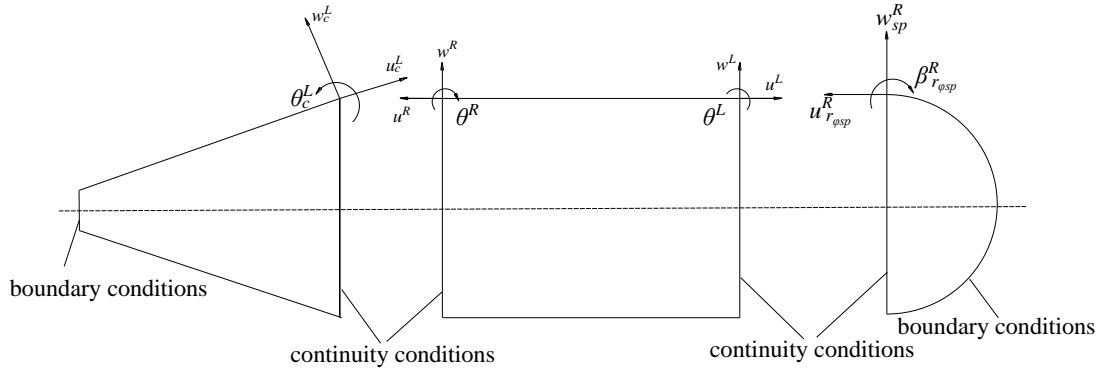
#### 2.3.2.1 Conditions at the Junction of Cylindrical Shell and Conical Shell

Considering the bulkhead, the displacements and forces continuity conditions at the junction of cylindrical shell and conical shell are given in Eq. (10).

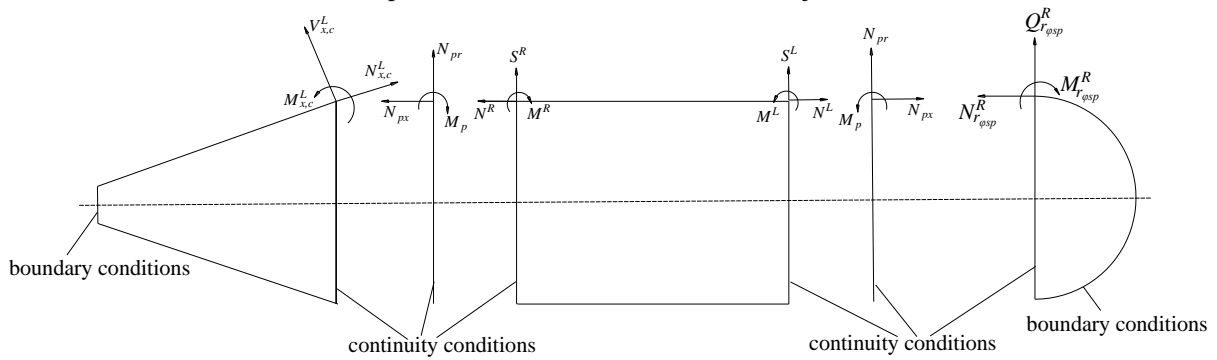
Parameters in Eq. (10) are displacements and internal forces of cylindrical shell and conical shell as

shown in Figure 3. The displacements and forces' detailed expressions can be found in references (5, 10). The subscripts 'c' and 'p' denote conical shell and bulkhead respectively.

$$\begin{cases} u^R = u_c^L \cos \alpha - w_c^L \sin \alpha \\ v^R = v_c^L \\ w^R = u_c^L \sin \alpha + w_c^L \cos \alpha \\ \theta^R = -\theta_c^L \end{cases} \quad \text{and} \quad \begin{cases} N_{x,c}^L \cos \alpha - V_{x,c}^L \sin \alpha = N_{px} + N^R \\ V_{x,c}^L \cos \alpha + N_{x,c}^L \sin \alpha = N_{pr} + S^R \\ N_{x\theta,c}^L = -N_{p\theta} + T^R \\ M_{x,c}^L = -M_p + M^R \end{cases} \quad (10)$$



(a) Displacements at C-C-S combined shell junctions



(b) Internal forces at C-C-S combined shell junctions

Figure 3 – Displacements and internal forces at C-C-S combined shell junctions

### 2.3.2.2 Conditions at the Junction of Cylindrical Shell and Spherical Shell

Considering the bulkhead, the displacements and forces continuity conditions at the junction of cylindrical shell and spherical shell are given as follows:

$$\begin{cases} u^L = u_{r\phi sp}^R \\ v^L = u_{\theta sp}^R \\ w^L = w_{sp}^R \\ \theta^L = -\beta_{r\phi sp}^R \end{cases} \quad \text{and} \quad \begin{cases} N^L = N_{px} + N_{r\phi sp}^R \\ S^L = N_{pr} + Q_{r\phi sp}^R \\ T^L = -N_{p\theta} + N_{r\phi sp \theta sp}^R \\ M^L = -M_p + M_{r\phi sp}^R \end{cases} \quad (11)$$

Parameters in Eq.(11) are displacements and internal forces of cylindrical shell and spherical shell as shown in Figure 3. The displacements and forces' detailed expressions can be found in references (5, 12).The subscripts 'r' and 'p' denote spherical shell and bulkhead respectively.

### 2.3.2.3 Conditions inside of the Cylindrical Shell and Conical Shell

Inside of the cylindrical shell, the cylindrical shell is divided into two segments by the ordinary ribs or large frame ribs or bulkheads as shown in Figure 2 and Figure 4 where continuity equations must be satisfied. The displacements of the two adjacent ends of the cylindrical shells must be equal, which can lead to the following relationships.

$$w^L = w^R, v^L = v^R, u^L = u^R, \theta^L = \theta^R \quad (12)$$

The superscripts 'L' and 'R' denote regions of the cylindrical shell to the left and right of the discontinuities under consideration.

The annular circular plate (i.e. ordinary rib or large frame rib), has one free edge at the inner radius ( $r=a_1$ ) where boundary conditions must be applied, ie:



The initial and final blocks  $[B_1]_{4 \times 8}$  and  $[B_{N_s}]_{4 \times 8}$  are expressed in terms of displacements and/or forces, depending on the boundary conditions at each end of the C-C-S combined shell. Combination of eight boundary conditions in 2.3.1 section can present arbitrary boundary conditions. Clamped, shear-diaphragm and free boundary conditions are considered in the following numerical Analysis. The  $4 \times 8$  matrix blocks  $[D_k(0)]_{4 \times 8}$  and  $[D_k(b_k)]_{4 \times 8}$  are the  $k$ th shell substructure's beginning and end displacements continuity conditions shown in 2.3.2 section. The  $4 \times 8$  matrix blocks  $[F_k(0)]_{4 \times 8}$  and  $[F_k(b_k)]_{4 \times 8}$  are the  $k$ th shell substructure's beginning and end forces continuity conditions shown in 2.3.2 section.  $b_k$  designates the length of the  $k$ th shell segment of the combined shell.

The undetermined coefficient vector  $\{A\}$  can be obtained by solving Eq. (18). Then substitute the  $k$ th segment solved coefficients into the  $k$ th segment shell's displacement functions, the vibration responses of the combined shell can be worked out.

### 3. RESULTS AND DISCUSSIONS

#### 3.1 Validity of ASM

The ASM model is developed to calculate the vibration responses of C-C-S combined shell for clamped-clamped(C-C) boundary, simply supported-simply supported (SD-SD) boundary, free-free (F-F) boundary with FEM results to show the validity of ASM model. The computation model is considered here as shown in Figure 1. The geometry and material properties of the C-C-S combined shell are listed in Table 2. The whole structure has the same material.

Table 2 – Geometry dimensions and material properties of the C-C-S combined shell

Name of parameters	Unit	Value	Name of parameters	Unit	Value
Radius of conical shell at small end	<i>m</i>	0.5	Width of frame rib	<i>m</i>	0.021
Radius of conical shell at big end (i.e. Radius of cylindrical shell and spherical shell)	<i>m</i>	3.5	Depth of frame rib	<i>m</i>	0.8
Length of conical shell	<i>m</i>	10.8	Position of frame rib	/	#50
Thickness of conical shell	<i>m</i>	0.016	Thickness of bulkhead	<i>m</i>	0.03
Length of cylindrical shell	<i>m</i>	48	Position of bulkhead	/	#18, #34, #66, #82, #98
Thickness of cylindrical shell	<i>m</i>	0.032	Position of driving force	/	#62
Length of spherical shell	<i>m</i>	3.5	Direction of driving force	/	radial direction
Thickness of spherical shell	<i>m</i>	0.03	Amplitude of driving force	<i>N</i>	1
Width of ordinary ribs	<i>m</i>	0.014	Density	<i>kg/m<sup>3</sup></i>	7800
Depth of ordinary ribs	<i>m</i>	0.25	Young's modulus	<i>Pa</i>	$2.1 \times 10^{11}$
Spacing of ordinary ribs	<i>m</i>	0.6	Poisson ratio	/	0.3

Considering the speed of FEM calculation, the calculated frequencies are range from 1Hz to 300Hz with 1Hz step.

The FE software ANSYS is used to calculate frequency responses of the C-C-S combined shell. In order to ensure the convergence of results calculated by FEM, three different kinds of meshes shown in Table 3 are used to calculate frequency responses of combined shell with the results shown in Figure 5(a). The ASM model is divided into different substructures which are also shown in Table 1. From Table 3 we can see that the number of substructures in ASM model is much less than the number of elements used in FEM models, and the calculation speed of ASM is much faster than that of FEM. Figure 5(a) shows that Mesh 2 which can achieve both high computation efficiency and adequate converged results in the range of calculation frequency is used in the following analysis.

In order to ensure the convergence of results calculated by ASM, The maximum circumferential wave numbers  $n_{\max}$  are offered as 10, 15, 20, 25 respectively. Figure 5(b) shows the comparison of mean square velocity level of the combined sell with four different maximum circumferential wave numbers. From above figure we can see that the ASM convergence is desirable in the range of calculation frequency when the maximum circumferential wave number is 20, which is used in the following ASM calculation.

Figure 6 shows the comparison of frequency response of the combined shell between ASM results and FEM results. As we can see from the figure, the results are in good agreement which show the

validity of ASM model.

Table 3 – FEM models with different meshes and shell substructure divisions of ASM models

Method	ASM	FEM		
Comparison of the items	Number of shell substructures	Number of elements		
		Mesh 1	Mesh 2	Mesh 3
Value	99	34563	62070	97059

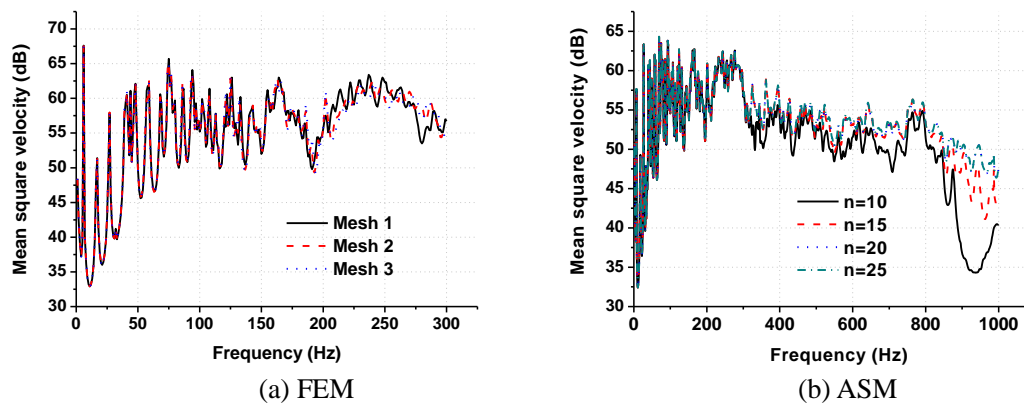


Figure 5 – Convergence analysis of the combined shell using FEM and ASM

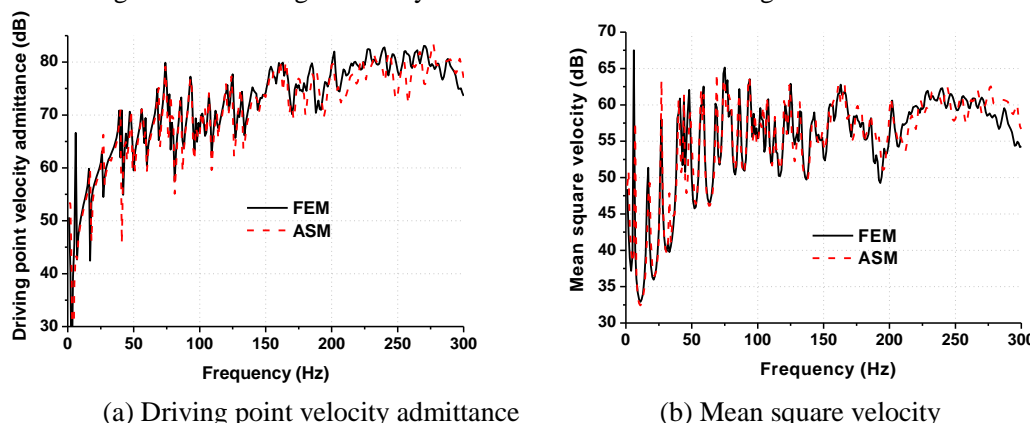


Figure 6 – Comparison on frequency response of C-C-S combined shell using FEM and ASM

### 3.2 Effect of Boundary Conditions

Figure 7 shows the comparisons on vibration characteristics of C-C-S combined shell with clamped, simply supported and free boundary conditions. It is observed that boundary conditions are of little influence on the vibration characteristics of combined shell in general, especially above 100Hz. Moreover, the vibrational curves with simply supported boundary condition are much closer to that of clamped boundary condition in the whole calculated frequency range. The small vibrational differences of three boundary conditions are the position of the first few resonant peaks in low frequency range (below 100Hz), and the first few resonant peaks shift to lower frequencies with the relaxation of boundary constraints.

## 4. CONCLUSIONS

ASM, which can be regarded as an effective semi-analytical and semi-numerical method, has been presented to analyze the vibration characteristics of C-C-S combined shell with arbitrary boundary conditions. In contrast with the FEM, the size of ASM final matrix is much smaller than the matrix formed in FEM, thus the calculation speed of ASM is much faster than that of FEM. Numerical calculations of ASM model show good agreement with the results calculated by FEM.

The influence of boundary conditions on vibration characteristics of combined shell is very small, especially at high frequencies. The small vibrational differences appear at the positions of resonant peaks in the low frequency range. More specifically, the first few resonant peaks shift to lower

frequencies with the relaxation of boundary constraints. This indicates that the influence of boundary conditions can be ignored at the high frequency.

ASM is capable of fast prediction of vibration characteristics of complex combined shell structure. It is applicable for complex structures with any boundary conditions, which can provide an analyzed method for calculation vibration response of multi-segmental complex shell.

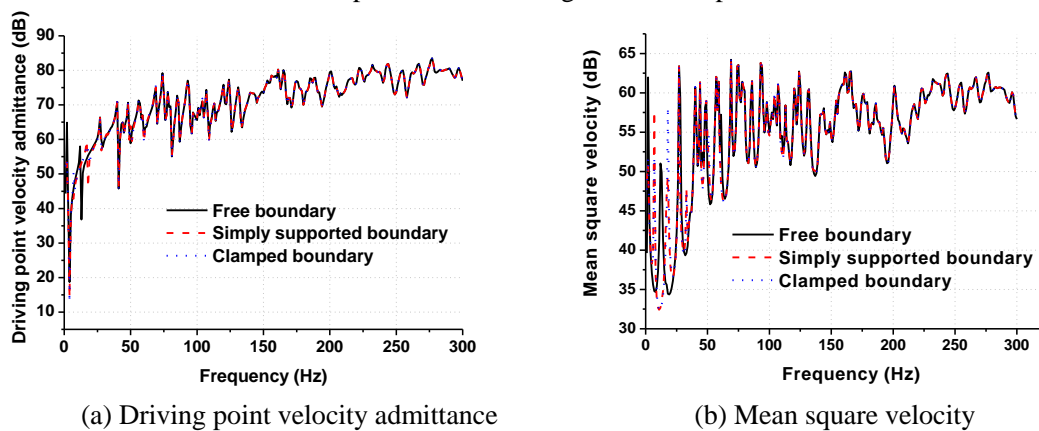


Figure 7 – Comparison on frequency response of C-C-S combined shell with three boundary conditions

## ACKNOWLEDGMENTS

The work in this paper is supported by the National Natural Science Foundation of China (51179071) and the China Scholarship Council (201208420328). Meanwhile, Prof. Jie Pan in the University of Western Australia is gratefully acknowledged for revising and correcting the paper.

## REFERENCES

1. Pan X, Tso Y, Juniper R. Active control of radiated pressure of a submarine hull. *Journal of Sound and Vibration*, 2008, 311(1-2): 224-242
2. Caresta M, Kessissoglou N.J. Structural and acoustic responses of a fluid-loaded cylindrical hull with structural discontinuities. *Applied Acoustics*, 2009, 70(7): 954-963
3. Caresta M, Kessissoglou N.J. Free vibrational characteristics of isotropic coupled cylindrical-conical shells. *Journal of Sound and Vibration*, 2010, 329(6): 733-751
4. Qu Y.G., Chen Y, Long X.H. A modified variational approach for vibration analysis of ring stiffened conical-cylindrical shell combinations. *European Journal of Mechanics A/Solids*, 2013,37: 200-215
5. Thein Wah, William C.L.Hu, Vibration analysis of stiffened cylinders including inter-ring motion. *The Journal of the Acoustical Society of America*, 1968, 43(5): 1005-1016
6. M.X.Chen, J.H.Wei, K.Xie, N.Q.Deng, G.X.Hou, Wave Based Method for Free Vibration Analysis of Ring Stiffened Cylindrical Shell with Intermediate Large Frame Ribs. *Shock and Vibration*, 2013, 20: 459-479
7. J.H.Wei, M.X.Chen, G.X.Hou, K.Xie, N.Q.Deng, Wave based method for free vibration analysis of cylindrical shell with non-uniform stiffener distribution. *Journal of Vibration and Acoustics*, 2013, 135(6):061011
8. Tso Y.K, Hansen C.H. Wave propagation through cylinder/plate junctions. *Journal of Sound and Vibration*, 1995, 186(3): 447-461
9. Caresta M, Kessissoglou N.J. Vibration of fluid loaded conical shells. *The Journal of the Acoustical Society of America*, 2008, 124(4): 2068-2077
10. Caresta M. Structural and acoustic responses of a submerged vessel. [PhD dissertation]. Sydney, Australia: University of New South Wales, 2009
11. Chen M, Zhang C, Tao X, Deng N. Structural and acoustic responses of a submerged stiffened conical shell. *Shock and vibration*, Volume 2014 (2014), Article ID 954253, 14 pages
12. Kalnins A. On vibrations of shallow spherical shells. *The Journal of the Acoustical Society of America*, 1961, 33(8), 1102-1107